Water Accessibility to the Tryptophan Indole N-H Sites of Gramicidin A Transmembrane Channel: Detection of Positional Shifts of Tryptophans 11 and 13 along the Channel Axis upon Cation Binding†

Teruhiko Maruyama and Hideo Takeuchi*

Pharmaceutical Institute, Tohoku University, Aobayama, Sendai 980-77, Japan

Received May 8, 1997⊗

ABSTRACT: Gramicidin A analogues, in which one of four Trp residues was selectively substituted by carbon-deuterated Trp, were incorporated into phospholipid liposomes and their Raman spectra were recorded in the absence and presence of Na^+. Detailed analyses of the Raman spectra have revealed the conformation, strength of hydrophobic interaction, and water accessibility of each individual Trp residue of the gramicidin transmembrane channel. The absolute value of the torsion angle $\chi^{2,1}$ about the $C_\alpha C_\beta - C_3C_2$ linkage is found to be 94° ± 6° in both the cation-free and Na^+-bound states. The Trp side chains are generally involved in strong hydrophobic interactions with the lipid acyl chains of the membrane and/or with another Trp residue. The water accessibility to the indole N_1H site is in the order Trp-15 > Trp-13 ≫ Trp-11 > Trp-9 in the cation-free state. In the Na^+-bound state, however, the water accessibility significantly decreases for Trp-13 and increases for Trp-11 without change for Trp-15 and -9. The site-specific changes of water accessibility are explained by a combination of positional shifts of Trp-13 and -11 toward the channel center and the channel mouth, respectively. Model building has shown that such positional shifts of Trp indole rings can be linked with deflections of amide C═O bonds toward the channel pore, suggesting a cation-induced conformational transition of the channel backbone structure.

Gramicidin A is an antibiotic pentadecapeptide that forms transmembrane channels permeable to monovalent cations and water (*1*−*3*). The amino acid sequence of this peptide is characterized by a high content of hydrophobic residues and an alternating arrangement of L- and D-amino acids: HCO-L-Val-Gly-L-Ala-D-Leu-L-Ala-D-Val-L-Val-D-Val-L-Trp-D-Leu-L-Trp-D-Leu-L-Trp-D-Leu-L-Trp-$NHCH_2CH_2$-OH (*4*). The structure of the gramicidin A transmembrane channel has been studied extensively for decades (for recent reviews, see refs *5* and *6*) and a model for the channel backbone structure has been proposed by Urry and co-workers (*7*−*9*). According to Urry's model, two monomers of gramicidin A are linked together at their formyl-N termini in an antiparallel linear arrangement and the head-to-head dimer spans the bilayer membrane. Each monomer forms a left-handed helix with 6.3 residues/turn and with the main-chain torsion angles close to those of β-sheet (left-handed $\beta^{6.3}$ helix). However, recent NMR studies in oriented lipid bilayers (*10*) and in multilamellar dispersions (*11*) have provided considerable evidence that requires revision of the helix sense from left-handed to right-handed. The right-handed $\beta^{6.3}$ helix is now generally accepted as the backbone structure of the gramicidin channel. Irrespective of the helix sense, a tunnel for ion transport (4 Å in diameter) is formed inside the peptide backbone of the $\beta^{6.3}$ helix and the side chains of hydrophobic amino acids protrude from the channel backbone, permitting interactions with the lipid membrane.

Among the amino acid residues of gramicidin A, four Trp residues at positions 9, 11, 13, and 15 have the largest side chains and the their bulky indole rings are considered to play a key role in the gramicidin−lipid interaction. The importance of the Trp residues in channel structure formation and cation transport has been demonstrated by the observation that replacement of one or more Trp residues with phenylalanine or tyrosine residues significantly reduces the cation conductance (*12*−*15*). Hydrophobic interactions with lipid acyl chains and electrostatic interactions with cations may be related to the functional importance of the Trp residues. Both the hydrophobic and electrostatic interactions depend on the orientations of the indole rings with respect to the channel axis as well as their axial (along the lipid bilayer normal) and radial (toward the surrounding lipid) positions. Determination of the orientations and positions of four Trp indole rings is an important step to understanding the molecular mechanism of ion transport through the gramicidin channel.

Several attempts have been made to determine the Trp indole ring orientations in the gramicidin channel. If the detailed structure of the channel helix backbone is known, the orientation of the indole ring of a Trp residue can be represented by a pair of two torsional angles, χ^1 about the $NC_\alpha - C_\beta C_3$ linkage and $\chi^{2,1}$ about the $C_\alpha C_\beta - C_3C_2$ linkage. Among the two torsional angles, the $\chi^{2,1}$ angle has been proposed to be close to ±90° for every Trp by using a relationship between the absolute value of $\chi^{2,1}$ and the frequency of an indole ring vibration that appears strongly in Raman spectra (*16*). Subsequent NMR studies on D- and/or ^{15}N-labeled gramicidin analogues in oriented lipid bilayers have proposed a number of possible pairs of χ^1 and $\chi^{2,1}$ that produce indole ring orientations consistent with the NMR orientational constraints (*17*−*19*). Very recently, a detailed analysis of the solid-state D- and ^{15}N-NMR data in terms of

† Supported in part by a Grant-in-Aid for Exploratory Research (08874062) from the Ministry of Education, Science, Sports and Culture of Japan.

⊗ Abstract published in *Advance ACS Abstracts,* August 15, 1997.

S0006-2960(97)01083-0 CCC: $14.00

the dipolar, quadrupolar, and chemical shift interactions has reduced the number of possible (χ^1, $\chi^{2,1}$) pairs to four for each Trp residue (*20*).

Additional information on the Trp orientations and positions can be obtained by analyzing the hydrogen−deuterium (H−D) exchange at the N_1H site of the indole ring. The water (D_2O) accessibility to the N_1H proton is considered to depend on the distance of the labile proton from the lipid membrane surface and the distance is a function of χ^1 and $\chi^{2,1}$ as well as of the axial position of the Trp residue. In a previous Raman study (*16*), we demonstrated that the water accessibility to indole N_1H sites decreases when the gramicidin channel is incorporated into thicker lipid membranes, suggesting that the H−D exchange rate serves as a measure of the distance of the N_1H proton from the membrane surface. In this study, we have examined H−D exchange kinetics of individual Trp residues in the gramicidin channel by replacing each Trp residue with a Trp isotopomer deuterated at the ring carbons (L-Trp-2,4,5,6,7-d_5, hereafter called dTrp[1]). This selective deuterium labeling has further enabled us to determine the $|\chi^{2,1}|$ angle and the strength of hydrophobic interaction of each Trp by Raman spectroscopy. Here we report the results of Raman spectral analysis of the water accessibility, conformation, and hydrophobic interaction of each individual Trp residue in the gramicidin channel incorporated into phospholipid bilayer membranes.

MATERIALS AND METHODS

Dilauroyl-L-α-phosphatidylcholine (DLPC, 99%) was purchased from Sigma Chemical Co. and used without further purification. L-Tryptophan was supplied by Ajinomoto Co. The carbon-deuterated tryptophan, dTrp, was prepared by repeated H−D exchange reactions in the dark at room temperature using trifluoroacetic anhydride dissolved in D_2O (2:1 v/v) as the exchange reagent (*21*). NMR spectra (500 MHz) showed 92.4% deuteration on the ring carbons. The amino and carboxyl groups of dTrp were protected with 9-fluorenylmethyl chloroformate (*22*) and pentafluorophenol- (*23*), respectively, to obtain 9-fluorenylmethoxycarbonyl-L-tryptophan-2,4,5,6,7-d_5 pentafluorophenol (Fmoc-L-dTrp-pfp). The protection methods were also used for preparation of Fmoc-D-Val-pfp and Fmoc-D-Leu-pfp. The other amino acid derivatives used for peptide synthesis were purchased from commercial suppliers.

Gramicidin A analogues selectively labeled with dTrp at position 9, 11, 13, or 15 (hereafter denoted GA-9dW, -11dW, -13dW, or -15dW) were prepared on a solid-phase peptide synthesizer (Pharmacia, Biolynx 4175) by the standard Fmoc method. The peptides were cleaved from the resin (Milligen, Pepsyn KA) with ethanolamine (*24*). Unlabeled gramicidin A was also synthesized by the same method. The cleaved peptide was purified and analyzed by HPLC (Jasco 880) on a gel-filtration column (Asahi, GS-320P) and a reversed-phase column (Nacalai, 5C18-AR). The retention time of purified peptide was identical to that of gramicidin A contained in natural gramicidin A′ (Sigma, a mixture of gramicidins A, B, and C) (*25*). The final products were further purified by recrystallization from methanol. ^{1}H NMR spectra (500 MHz) were recorded in dimethyl sulfoxide-d_6 to determine the degree of deuteration on the indole ring carbons: 87% for GA-13dW and 90% for the other dTrp-labeled gramicidin analogues. No Raman bands due to partially deuterated indole rings were detected for the gramicidin A analogues. Deuteration at the indole N_1H sites of gramicidin A and its dTrp-labeled analogues was performed by repeated recrystallization from CH_3OD. The Raman spectra of N-deuterated gramicidins in the solid state showed practically complete H → D exchange at the indole N_1H sites.

Preparation of gramicidin-incorporated liposomes and Raman spectral measurements were performed as described previously (*16*). Briefly, 2.0 mg (1.1 μmol) of peptide and 5.5 mg of DLPC (molar ratio ∼1:8) were dissolved in 5 mL of 2,2,2-trifluoroethanol (99%), which is known to be a good solvent to convert gramicidin A into the proper channel conformation (*26*−*28*). It is also known that gramicidin A readily forms the channel conformation in DLPC liposomes (*29*). The solution of peptide−lipid mixture was spread as a thin layer onto the wall of a round-bottom flask by drying under vacuum. After complete removal of the solvent, the lipid layer was hydrated with deionized water (3 mL) under vortexing. For preparation of liposomes in the presence of Na^+, 3 mL of 20 mM NaCl aqueous solution was used instead of deionized water. The opaque suspension of lipid was sonicated for 10−20 min by using an ultrasonic generator. The hydration and sonication were carried out at 10 °C, which is above the gel to liquid-crystalline phase transition temperature of DLPC (3.3 °C) (*30*). After sonication, the suspension was centrifuged to sediment traces of multilamellar aggregate and then the supernatant was concentrated at 1 °C to a volume of ∼0.1 mL by centrifugal filtration with a membrane filter (Amicon, Centriflo CF25, molecular weight cutoff 25 000). For H−D exchange experiments, a large excess (more than 30 times in volume) of D_2O (containing 20 mM NaCl when examining cation effects) was added to the liposome suspension, which was subsequently concentrated to ∼0.1 mL by centrifugal filtration in a closed container. The concentrated liposome suspension was sealed in a glass capillary and mounted on a brass block thermostated at 1 °C with a constant temperature circulating bath.

Raman spectra were recorded on a Jasco CT-80D spectrometer equipped with an Ar^+ laser (488 nm) and with an intensified diode array detector (Princeton Instruments, D/SIDA-700IG). Wavenumber calibration was made by using the spectrum of indene and peak wavenumbers of sharp Raman bands were reproducible to within ±0.5 cm^{-1}. The spectra to be reported here are the averages of spectra measured for more than three independently prepared samples.

RESULTS

Raman Bands of Trp and dTrp. Figure 1 shows the Raman spectra of amino acid Trp and dTrp in H_2O and D_2O solutions. The concentration of Trp or dTrp is 50 mM and the intensity of each spectrum is scaled by using the 934 cm^{-1} Raman band of 50 mM $NaClO_4$ added to the solution as an internal intensity standard. The frequencies of the Trp band labeled ω3 at 1551 cm^{-1} (spectrum A) and of the corresponding band of dTrp, ω_d3, at 1527 cm^{-1} (spectrum C) have been shown to serve as markers of the absolute value

[1] Abbreviations: dTrp, L-tryptophan-2,4,5,6,7-d_5; DLPC, dilauroyl-L-α-phosphatidylcholine; Fmoc, 9-fluorenylmethoxycarbonyl; pfp, pentafluorophenol; GA-*x*dW, gramicidin A analogue labeled with dTrp at position *x*.

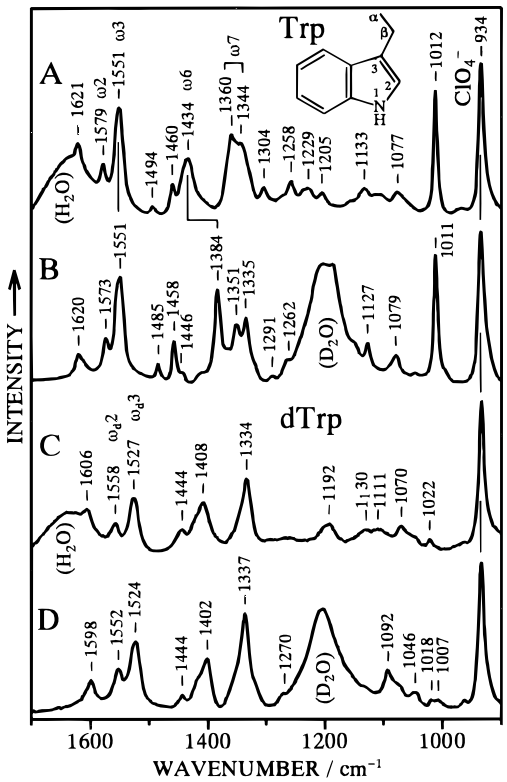

FIGURE 1: Raman spectra of amino acid L-Trp in H_2O (A) and D_2O (B) solutions and of dTrp (L-Trp-2,4,5,6,7-d_5) in H_2O (C) and D_2O (D) solutions. The concentration of the amino acid is 50 mM. The 934 cm^{-1} band is due to ClO_4^- (50 mM) added as an internal intensity standard.

of $\chi^{2,1}$ in a range of 60−120° (*31*, *32*):

$$\nu(\omega 3) = 1542 + 6.7(\cos 3|\chi^{2,1}| + 1)^{1.2} \quad (1)$$

$$\nu(\omega_d 3) = 1514 + 7.5(\cos 3|\chi^{2,1}| + 1)^{1.2} \quad (2)$$

where ν stands for the vibrational frequency in units of reciprocal centimeters. The $\omega 3$ band is expected to overlap a weak band of dTrp at 1558 cm^{-1} ($\omega_d 2$, spectrum C) in dTrp-labeled gramicidins. However, the Raman cross-section of the $\omega_d 2$ mode is about $^1/_7$ that of the $\omega 3$ mode (compare spectra A and C) and therefore the contribution of the $\omega_d 2$ band to the Raman intensity around 1550 cm^{-1} may be neglected for gramicidin analogues in which dTrp is substituted for only one of the four Trp residues. The $\omega 3$ frequency is thus regarded as a marker of the average $|\chi^{2,1}|$ angle for the unlabeled three Trp residues. On the other hand, the $\omega_d 3$ band of dTrp is not overlapped by any Raman bands of Trp and the $\omega_d 3$ frequency can be used to determine the $|\chi^{2,1}|$ angle of the dTrp residue in labeled gramicidins.

The doublet at 1360/1343 cm^{-1} in spectrum A of Figure 1 is known to arise from Fermi resonance between a fundamental $\omega 7$ and one or two combinations of the indole ring out-of-plane vibrations (*33*). Hydrophobic interactions of the indole ring with surrounding molecules affect the frequencies of the combinations and the intensity ratio of the doublet changes depending on the separation in frequency between the fundamental and combinations. As a result, the intensity ratio of the high- to low-frequency components I_{high}/I_{low} becomes larger for stronger hydrophobic interactions (*33*, *34*). For dTrp, the corresponding vibration appears as a singlet at 1334 cm^{-1} (spectrum C) due to removal of the

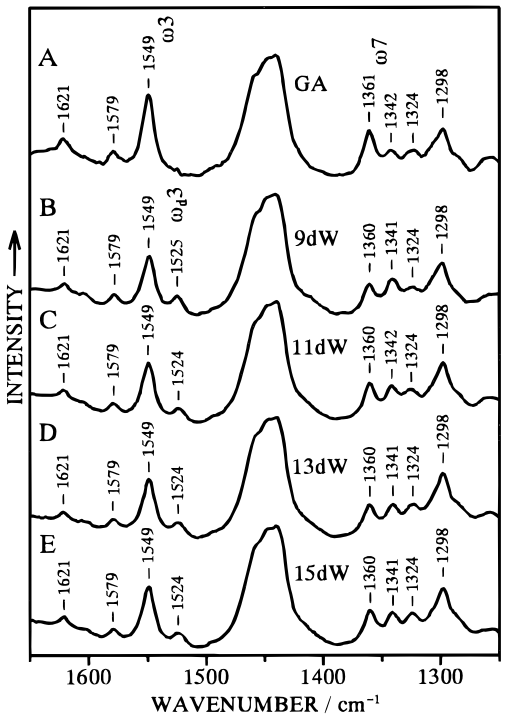

FIGURE 2: Raman spectra of gramicidin channels incorporated into DLPC liposomes: (A) unlabeled gramicidin A, (B) GA-9dW, (C) GA-11dW, (D) GA-13dW, and (E) GA-15dW.

Fermi resonance, and its intensity is no longer expected to serve as a measure of hydrophobic interaction. For dTrp-labeled gramicidins, the intensity of the high-frequency component at 1360 cm^{-1} may be used to measure the strength of hydrophobic interaction of unlabeled Trp residues.

Deuteration at the indole N_1H site causes only small frequency shifts (<10 cm^{-1}) of the dTrp Raman bands (compare spectra C and D), and the Raman bands of dTrp and N-deuterated dTrp will overlap each other when both the N_1-H and N_1-D forms coexist. Accordingly, it is difficult to directly monitor the N-deuteration of the dTrp residue in labeled gramicidins. On the other hand, the $\omega 6$ mode of Trp shows a large frequency downshift from 1434 to 1384 cm^{-1} (spectra A and B). This large shift reflects a significant contribution of the N_1-H bending vibration to the $\omega 6$ mode (*35*). The 1384 cm^{-1} band of N-deuterated Trp falls into a window region of Raman spectra of proteins and peptides, and the intensity of this Raman band has been used to measure H−D exchange kinetics of Trp residues (*16*, *34*, *36*). This band can also be used to monitor the H−D exchange of three unlabeled Trp residues in singly dTrp-labeled gramicidins. In evaluating the number of N-deuterated Trp residues from the Raman intensity of the 1384 cm^{-1} band, the $\omega 3$ band of Trp can be used as an intensity reference because the $\omega 3$ intensity is insensitive to N-deuteration (see spectra A and B).

Raman Spectra of dTrp-Labeled Gramicidins Incorporated into Liposomes. Figure 2 compares Raman spectra of dTrp-labeled gramicidins incorporated into DLPC liposomes with that of unlabeled gramicidin. In the spectra, the strong and broad Raman band around 1450 cm^{-1} and a band peaking at 1298 cm^{-1} are ascribed to the CH_2 scissors and twisting modes, respectively, of the lipid acyl chain (*16*). Weak Raman bands of gramicidin in these frequency regions are obscured by the overlap of the lipid Raman bands. In the

other frequency regions shown, all the prominent Raman bands are assigned to Trp or dTrp residues.

(1) $\chi^{2,1}$ Torsion Angle. The conformation maker band ω3 is observed at 1549 cm^{-1} for every one of unlabeled and dTrp-labeled gramicidins, indicating that the average $|\chi^{2,1}|$ angle for any combinations of three Trp residues is 91° ± 3°. The standard error (±3°) is estimated from the accuracy of wavenumber determination, ±0.5 cm^{-1}, and the uncertainty of the $\nu(\omega 3) - |\chi^{2,1}|$ relationship given by eq 1. Further information on the $\chi^{2,1}$ angles of individual Trp residues is provided by the frequency of the ω_d3 band of dTrp. The ω_d3 band is observed at 1525 cm^{-1} for GA-9dW and at 1524 cm^{-1} for GA-11dW, -13dW, and -15dW. By applying eq 2 to the ω_d3 frequencies, the $|\chi^{2,1}|$ angle is estimated to be 97° ± 3° for the Trp residue at position 9 (Trp-9) and 95° ± 3° for the other Trp residues (Trp-11, -13, and -15). Combining the estimated ranges for $|\chi^{2,1}|$, it may be safe to say that $|\chi^{2,1}|$ is in a range of 94° ± 6° for every Trp residue in the gramicidin channel. The $|\chi^{2,1}|$ range found here confirms the previous proposal that every Trp has a $\chi^{2,1}$ angle close to ±90° (*16*).

(2) Hydrophobic Interactions. As described above, the intensity ratio I_{high}/I_{low} of the ω7 doublet is greater for stronger hydrophobic interactions of Trp residues. In the spectrum of unlabeled gramicidin (Figure 2A), the high-frequency component at 1361 cm^{-1} is much stronger than the low-frequency component at 1342 cm^{-1}, indicating that all or most Trp residues in the gramicidin channel are involved in strong hydrophobic interactions (*16*). Upon replacement of one of the four Trp residues with dTrp, I_{high} is expected to decrease because of the absence of any Raman bands around 1360 cm^{-1} for dTrp, while I_{low} is expected to increase due to the overlap of a dTrp band at 1334 cm^{-1} (see spectrum C in Figure 1). The decrease of I_{high} indicates the contribution from the Trp residue that is replaced by dTrp. When we take the ω3 band as an intensity reference, the decrease of I_{high} is largest for GA-9dW and smallest for GA-11dW (spectra B−E in Figure 2). This is also the case when we take the strong lipid band around 1450 cm^{-1} as another intensity reference. The strength of hydrophobic interaction is in the order Trp-9 > Trp-13 ≈ Trp-15 > Trp-11, though even Trp-11 is involved in significant hydrophobic interactions.

(3) H−D Exchange at the Indole N_1H Site. To measure the H−D exchange rate, gramicidin-incorporated liposomes were first prepared in H_2O and then suspended in D_2O as described in Materials and Methods. Since gramicidin channels are highly permeable to water (*3*), H_2O molecules inside the liposomes will be readily replaced with D_2O molecules by changing the dispersion medium from H_2O to D_2O. Then, D_2O molecules penetrate into the lipid bilayer of liposome from the inside and outside surfaces (*37*, *38*). Trp N_1H protons are expected to be replaced with deuterium atoms if D_2O molecules are accessible to the N_1H sites.

The Raman spectra of liposomes suspended in D_2O were recorded at time intervals to monitor the H−D exchange at the indole N_1H sites. Figure 3 shows the Raman spectra of GA-11dW-incorporated liposomes recorded 3 (D), 5 (C), and 7 (B) hours after suspension in D_2O. The 1386 cm^{-1} band is characteristic of N-deuterated Trp and its intensity increases progressively with time. The top trace (A) in the figure shows the spectrum of liposomes prepared in D_2O and containing GA-11dW whose labile hydrogen atoms, including the N_1H protons, were exchanged with CH_3OD in advance. The spectrum of fully H−D-exchanged GA-11dW corresponds to what would be observed if the GA-11dW-incorporated liposomes were kept in D_2O for an infinitely long period of time and the indole rings of Trp-9, -13, and -15 were all N-deuterated. Similar H−D exchange experiments have also been done for liposomes containing GA-9dW, -13dW, and -15dW.

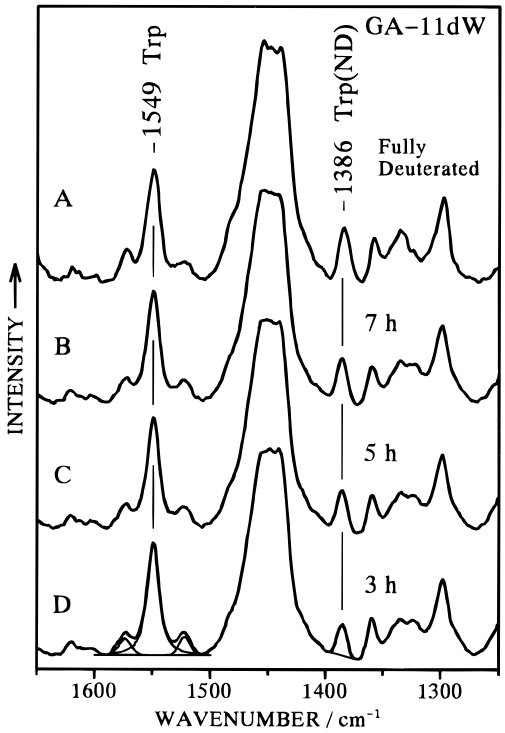

FIGURE 3: Raman spectra of GA-11dW incorporated into DLPC liposomes and suspended in D_2O: (A) Fully N-deuterated prior to the incorporation into liposomes, (B) 7 h after the dispersion medium was changed from H_2O to D_2O, and (C) 5 h after the medium exchange, (D) 3 h after the medium exchange.

As described above, the intensity of the 1549 cm^{-1} (ω3) Raman band of Trp is not affected by N-deuteration and serves as an intensity reference to measure the intensity increase of the 1386 cm^{-1} band upon N-deuteration. We have examined the integrated intensities of the 1549 and 1386 cm^{-1} bands by fitting each band to a sum of Gaussian and Lorentzian bands as illustrated with thin lines in spectrum D of Figure 3. For liposomes containing fully H−D-exchanged GA-9dW, -11dW, -13dW, or -15dW, the intensity ratio I(1386)/I(1549) was found to be nearly constant (0.305 ± 0.007). This finding indicates that the intrinsic ratio of I(1386)/I(1549) of a fully N-deuterated Trp residue does not depend on its location in the gramicidin channel, and therefore I(1386)/I(1549) is a good measure of N-deuteration for three Trp residues in each dTrp-labeled gramicidin. For example, I(1386)/I(1549) in spectrum D of Figure 3 is ∼50% of that in spectrum A, indicating that about half of the three unlabeled Trp residues (Trp-9, -13, and -15) are N-deuterated at a time of 3 h after suspension in D_2O. The number of N-deuterated Trp side chains thus obtained is plotted in Figure 4A as a function of time for GA-9dW, -11dW, 13-dW, and -15dW.

At a given time of observation, the number of N-deuterated Trp side chains, N_m, in GA-*m*dW is related to the percentage of N-deuteration, p_i, of the Trp residue at position i ($\neq m$):

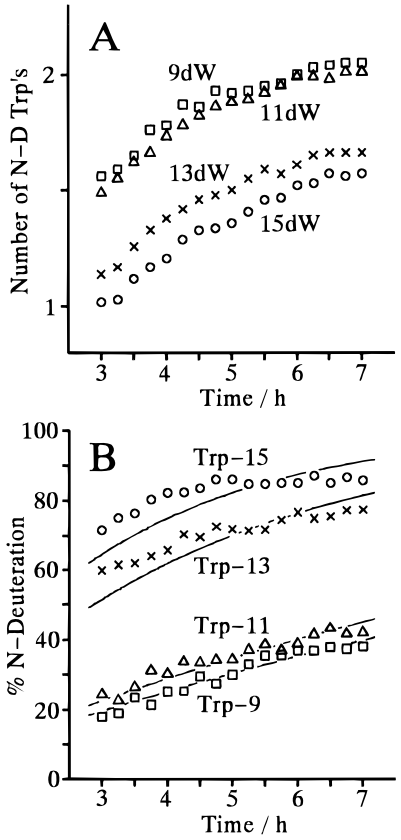

FIGURE 4: H−D exchange kinetics of dTrp-labeled gramicidin channels: (A) Number of N-deuterated Trp side chains per gramicidin monomer for GA-9dW (□), GA-11dW (△), GA-13dW (×), and GA-15dW (○); (B) percentages of N-deuteration of Trp-9 (□), Trp-11 (△), Trp-13 (×), and Trp-15 (○). Both are plotted as a function of time after suspension in D_2O. The curves in panel B show least-squares fits.

$$N_m = \sum_{i \neq m} p_i/100 \qquad (3)$$

By combining such equations for $m = 9$, 11, 13, and 15, p_i can be computed by

$$p_i = 100[(\sum_m N_m)/3 - N_i] \qquad (4)$$

The p_i values obtained from eq 4 are plotted in Figure 4B as a function of time. The curves in Figure 4B represent least-squares fits with single-exponential functions. The half-times for H−D exchange obtained by the least-squares analysis are listed in Table 1. Trp-15 exchanges with water (D_2O) with a half-time of 2.01 h, which indicates that the N_1H proton of Trp-15 is accessible to water (D_2O) but not exposed to the aqueous phase because exposed Trp shows much faster H−D exchange (*34*, *36*). The H−D exchange of Trp-13 is a little slower (half-time 2.88 h) than that of Trp-15. Trp-13 must be more buried in the hydrophobic region of the bilayer. In contrast to Trp-15 and -13, Trp-11 and -9 have very long half-times (8−10 h). Such slow exchange indicates that the N_1H sites of these Trp residues are deeply buried in the hydrophobic region of the lipid bilayer and hardly accessible to water.

(4) Effects of Cation Binding. To investigate the effects of cation binding on the gramicidin channel structure, we have prepared liposomes containing dTrp-labeled gramicidins in the presence of 20 mM NaCl. Figure 5 shows the Raman spectra of such liposomes. The ω3 conformation marker band of Trp is observed at 1549 cm^{-1} for all the dTrp-labeled gramicidins, as was observed in the absence of Na^+. The difference in the ω_d3 frequency is also small between the cation-free and Na^+-bound states, suggesting that the $|\chi^{2,1}|$ torsion angle remains in the 94° ± 6° range for all the Trp residues even in the presence of Na^+. The effect of Na^+ binding on the intensity of the 1360 cm^{-1} band is also marginal (compare Figures 2 and 5). It is concluded that the hydrophobic interactions of the Trp residues are not significantly affected by the Na^+ binding, the interaction being strongest for Trp-9 and weakest for Trp-11.

Table 1: Deuterium Exchange Kinetics of the Tryptophan N_1H Protons of Gramicidin A Incorporated into DLPC Liposomes

	half-time for exchange[a] (h)			
state	Trp-9	Trp-11	Trp-13	Trp-15
cation-free	9.56 ± 0.14	8.13 ± 0.13	2.88 ± 0.07	2.01 ± 0.07
Na^+-bound	9.42 ± 0.14	4.64 ± 0.11	4.07 ± 0.08	1.96 ± 0.06

[a] Obtained by the least-squares analysis using a function $1 - \exp(-t/\tau)$, where t is the time (hours) and τ ln 2 is the half-time for exchange.

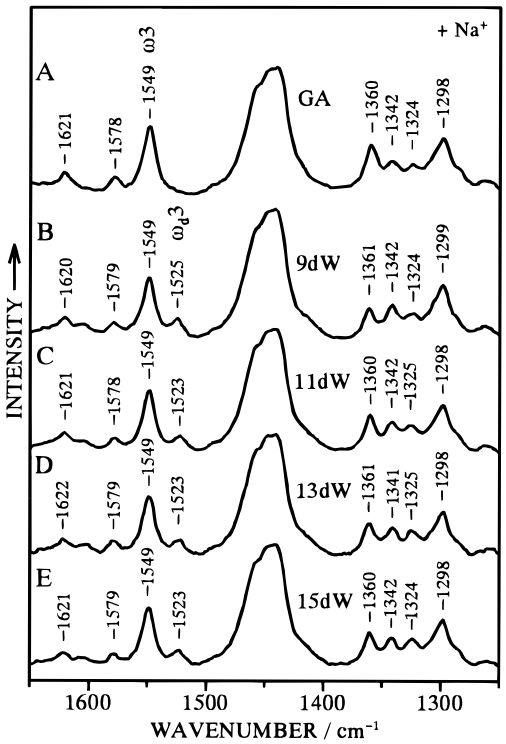

FIGURE 5: Raman spectra of gramicidin channels incorporated into DLPC liposomes in the presence of 20 mM NaCl: (A) unlabeled gramicidin A, (B) GA-9dW, (C) GA-11dW, (D) GA-13dW, and (E) GA-15dW.

Marked effects of the Na^+ binding are seen on the H−D exchange at the indole N_1H site. Figure 6A plots the number of N-deuterated Trp residues as a function of time for dTrp-labeled gramicidins in the presence of Na^+. The degree of N-deuteration for each Trp residue at a given time is obtained from the plots by using eq 4. The time courses of N-deuteration for Trp-9, -11, -13, and -15 are shown in Figure 6B and the half-times for H−D exchange are compared with those in the absence of cations in Table 1. For Trp-9 and -15, the half-time is not affected by Na^+ within the experimental error. In contrast, the Na^+ binding causes significant changes in the half-time from 8.13 to 4.64 h for Trp-11 and from 2.88 to 4.07 h for Trp-13. The N_1H site

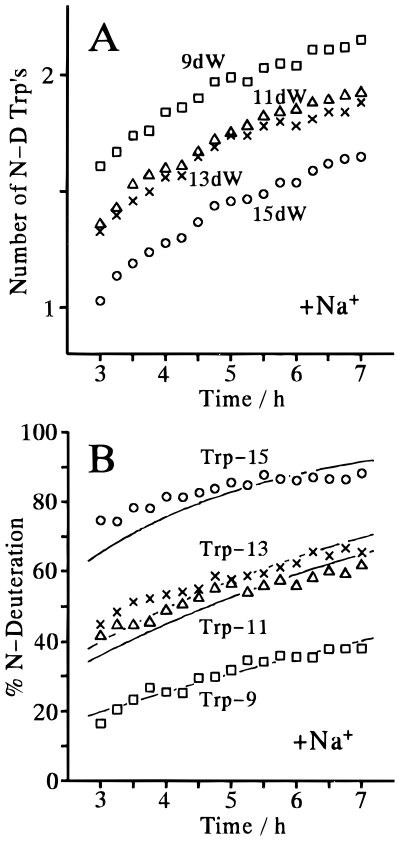

FIGURE 6: H−D exchange kinetics of dTrp-labeled gramicidin channels in the presence of 20 mM NaCl: (A) Number of N-deuterated Trp side chains per gramicidin monomer for GA-9dW (□), GA-11dW (△), GA-13dW (×), and GA-15dW (○); (B) percentages of N-deuteration of Trp-9 (□), Trp-11 (△), Trp-13 (×), and Trp-15 (○). Both are plotted as a function of time after suspension in D_2O. The curves in panel B show least-squares fits.

of Trp-11 becomes more accessible to water in the presence of Na^+, whereas that of Trp-13 becomes less accessible.

DISCUSSION

The Raman spectra of dTrp-labeled gramicidin analogues have provided information on the $|\chi^{2,1}|$ torsion angle, strength of hydrophobic interaction, and water accessibility for each individual Trp residue of the gramicidin channel. The $|\chi^{2,1}|$ torsion angle is found to be 94° ± 6° for every Trp residue both in the absence and presence of Na^+. The Trp indole rings are generally involved in strong hydrophobic interactions and the strength of hydrophobic interaction remains practically unchanged in the presence of Na^+. The water accessibility to the indole N_1H site is in the order Trp-15 > Trp-13 ≫ Trp-11 > Trp-9, the large gap between Trp-13 and -11 being characteristic of the cation-free state of the gramicidin channel. In the presence of Na^+, the water accessibility changes to the order Trp-15 ≫ Trp-13 ≥ Trp-11 ≫ Trp-9 due to significant decrease and increase for Trp-13 and -11, respectively. On the basis of these Raman data, we will discuss the orientations and positions of individual Trp side chains in the cation-free and Na^+-bound states of the gramicidin channel.

Cation-Free State. D- and ^{15}N-NMR analysis of uniformly oriented gramicidin channels has revealed constraints for the Trp indole ring orientations with respect to the channel axis, and only four pairs of χ^1 and $\chi^{2,1}$ for each Trp residue are found to produce the indole ring orientations consistent with

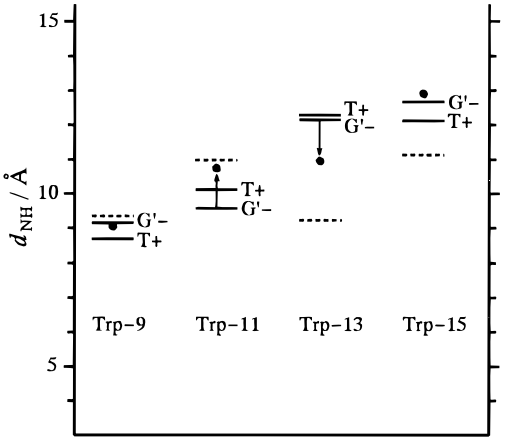

FIGURE 7: Distance of the N_1H proton (d_{NH}), measured along the channel axis from the head-to-head junction of the gramicidin dimer: Solid line, model 1; broken line, model 2; dot, model 3. For the details of the models, see text. The arrows indicate possible changes in d_{NH} of Trp-11 and -13 upon binding of Na^+ to the channel.

the NMR data (*20*). Although the χ^1 and $\chi^{2,1}$ values in the possible conformations slightly differ from residue to residue, χ^1 is in a range of −65° ± 7° or 170° ± 5° and $\chi^{2,1}$ is in a range of −89° ± 8°, −49° ± 3°, 89° ± 8°, or 49° ± 3° with the limitation that the negative χ^1 makes pairs only with the negative $\chi^{2,1}$ and vice versa (*20*). The conformations with $\chi^{2,1} = -49° \pm 3°$ or 49° ± 3° are, however, strongly disfavored by the present Raman finding that $|\chi^{2,1}|$ is 94° ± 6°. Accordingly, only two conformations remain possible for each Trp: $(\chi^1, \chi^{2,1}) = (-65° \pm 7°, -89° \pm 8°)$ and (170° ± 5°, 89° ± 8°). By adopting the notations G′ for $\chi^1 \approx -60°$, T for $\chi^1 \approx 180°$, + for $\chi^{2,1} \approx 90°$, and − for $\chi^{2,1} \approx -90°$, the possible conformations are represented by G′− and T+.

Water accessibility to the Trp N_1H site can be correlated with the position of the N_1H proton in the bilayer membrane as demonstrated previously (*16*). N_1H protons buried deeply in the hydrophobic region of the lipid bilayer membrane will be hardly accessible to water, whereas those closer to the membrane surface are expected to have higher possibilities to encounter the water molecules penetrating from the outer aqueous phase and to exchange protons. In order to interpret the H−D exchange kinetics of individual Trp residues, we have calculated the axial positions of N_1H protons for individual Trp residues in the G′− and T+ conformations. In the calculation, we used the χ^1 and $\chi^{2,1}$ angles proposed by Hu et al. for individual Trp residues (*20*) and the main-chain torsion angles (ϕ, ψ, ω) proposed by Ketchem et al. (*18*) for a right-handed $\beta^{6.3}$-helix of gramicidin A. The other structural parameters, bond lengths and angles, were taken from the literature (*39*).

Figure 7 shows the distances, d_{NH}, of the N_1H protons, measured along the helix axis, from the center of head-to-head dimer junction, which was assumed at 0.5 Å from C_α of Val-1 toward the bilayer interior (*40*). Larger d_{NH} values indicate shorter distances from the membrane surface. For Trp-13, d_{NH} is practically the same for the G′− and T+ conformations and distinction of the two conformations cannot be made by the water accessibility. The water accessibility of Trp-15 is higher than that of Trp-13 (Table 1), and this fact is accounted for by assuming that Trp-15 takes the G′− conformation because the N_1H proton of Trp-

15 is closer to the membrane surface than that of Trp-13 only in this conformation. Although the high water accessibility of Trp-15 suggests close proximity of this residue to the membrane surface, Raman spectra have indicated strong hydrophobic interactions of Trp-15. Trp-15 is separated from Trp-9 by one helix pitch on the $\beta^{6.3}$-helix and stacking interactions take place when both Trp residues are in the G′− conformation (*41*). The strong hydrophobic interaction of Trp-15 is likely to arise, at least partly, from stacking with Trp-9 in the G′− conformation. The stacking of Trp-15 with Trp-9 is consistent with the strongest hydrophobic interaction of Trp-9 revealed by Raman spectroscopy, with restricted librational motions of the two indole rings observed in NMR spectra (*20*), and with the presence of a short-lifetime component in Trp fluorescence decay (*42*).

The half-time for H−D exchange of Trp-11 is longer than that of Trp-9 by 15% (Table 1), suggesting a small rise in d_{NH} on going from Trp-9 to Trp-11. The N_1H proton of Trp-11 in the G′− conformation is closer to the membrane surface only by 0.4 Å than that of Trp-9 in the G′− conformation and this may explain the small difference in the H−D exchange rate. Accordingly, it is probable that Trp-11 is also in the G′− conformation. Hu and Cross (*41*) have proposed that all the Trp residues take the same conformation because the same tangential components of the indole dipole moments would facilitate cation transit on a helical path. Tentatively, we also assume that Trp-13 takes the same (G′−) conformation as the other Trp residues. The gramicidin channel model, in which four Trp residues in the G′− conformation are attached to the right-handed helix backbone of Ketchem et al. (*18*), corresponds to the most preferred structure of Hu and Cross (*41*). This model (hereafter called model 1) is fully consistent with the Raman data on the conformations, hydrophobic interactions, and water accessibilities of individual Trp residues in the absence of cations.

Very recently, Tian et al. (*43*) have proposed a refined model based on the D-, ^{15}N-, and ^{13}C-NMR spectra of aligned lipid bilayer preparations of the gramicidin channel. In the model (model 2), all Trp residues take the G′− conformation but the main-chain torsion angles (ϕ, ψ, ω) differ from those proposed by Ketchem et al. (*18*) and adopted in model 1. The d_{NH} values calculated with the main-chain torsion angles of model 2 are shown in Figure 7 with broken lines. The changes in main-chain torsion angle produce a very small d_{NH} of Trp-13, which is comparable to that of Trp-9. The order of d_{NH} calculated for model 2 is inconsistent with the order of water accessibility revealed here. The present Raman data support model 1 for the gramicidin channel structure, at least in the absence of cations.

Na^+-Bound State. In the presence of Na^+, the water accessibility of Trp-13 decreases and that of Trp-11 increases to comparable levels, while those of Trp-9 and -15 remain unchanged (Table 1). This observation indicates that Trp-11 becomes more accessible to water with an increase in d_{NH} and Trp-13 becomes less accessible with a decrease in d_{NH}. Since the changes in water accessibility are localized at Trp-11 and -13, they are not ascribed to structural changes of lipid bilayer in the presence of Na^+. If Na^+ bound to polar head groups of the bilayer membrane and affected the membrane structure, the water accessibility of Trp-15, which is closest to the membrane surface, would have changed significantly. Actually, however, it is known that Na^+ neither

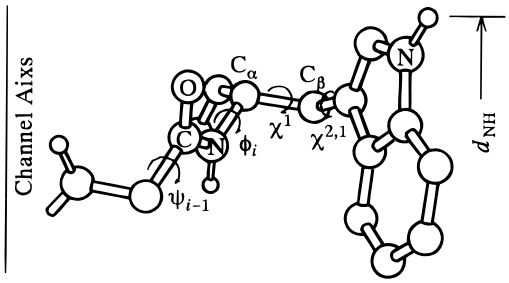

FIGURE 8: Torsion angles that may affect the indole N_1H position (d_{NH}) of a Trp residue in the gramicidin channel. The channel axis is vertical and the channel mouth is located at the top of the figure.

interacts strongly with the phosphatidylcholine polar head group (*44*) nor affects the acyl chain conformation of phospholipid (*45*). There must be some structural changes of the gramicidin channel associated with the binding of Na^+.

The orientational constraints for the Trp indole rings provided by the NMR analysis also apply for Na^+-bound gramicidin (*20*, *43*). The present Raman data have shown that $|\chi^{2,1}|$ angles are practically the same in the cation-free and Na^+-bound states. Accordingly, only the G′− and T+ conformations are possible for each Trp in the presence of Na^+ as is in the absence of cations. Conformational transitions from G′− to T+, however, fail to account for the large changes in d_{NH}, in particular for Trp-13 (see Figure 7). Another possibility is that the χ^1 and/or $\chi^{2,1}$ angles change to a small extent upon binding of Na^+. As shown in Figure 8, the d_{NH} is close to the maximum value for the rotation around the $\chi^{2,1}$ axis and a small change of the $\chi^{2,1}$ angle does not affect the d_{NH}. Rotation about the χ^1 axis is not very effective to change the d_{NH} either (20° rotation for a 1 Å change in d_{NH}). If χ^1 changes by 20°, the indole ring significantly reorients with respect to the channel axis, which is inconsistent with the NMR finding that any significant reorientation of the indole rings takes place upon binding of Na^+ (*20*, *43*). The changes in d_{NH} of Trp-11 and -13 cannot be explained by assuming changes in indole ring orientation.

Another factor that may affect the d_{NH} value is a shift of the indole ring along the channel axis. Such an axial shift can be produced by changing the ϕ angle of a Trp residue at position i (ϕ_i) and the ψ angle of the preceding residue (ψ_{i-1}). As shown in Figure 8, rotation about the ϕ_i axis alters the direction of the $C_\alpha-C_\beta$ bond to which the indole ring is attached, while rotation about the ψ_{i-1} axis makes a shift of the C_α atom along the channel axis. If both rotations take place in a concerted manner, it is possible for the Trp indole ring to move along the channel axis without significant reorientation of the ring. Effects of variation in ϕ_i and ψ_{i-1} are demonstrated in the d_{NH} values calculated with the (ϕ, ψ, ω) angles of model 2 (see Figure 7). The helix backbone structures in models 1 and 2 were both derived from the NMR orientational constraints for the amide N−H and N−C(=O) bonds but they differ largely in (ϕ_i, ψ_{i-1}) angles, as shown in Table 2. The differences in d_{NH} between models 1 and 2 (Figure 7) may be attributed to the differences in the ϕ_i and ψ_{i-1} angles.

We have searched the ϕ_i and ψ_{i-1} angles that produce d_{NH} values consistent with the water accessibility data. The conformational search was carried out by changing the ϕ_i and ψ_{i-1} angles (i = 9, 11, 13, and 15) independently in a range from −90° to −140° with a 5° step. The other structural parameters were assumed to be the same as in

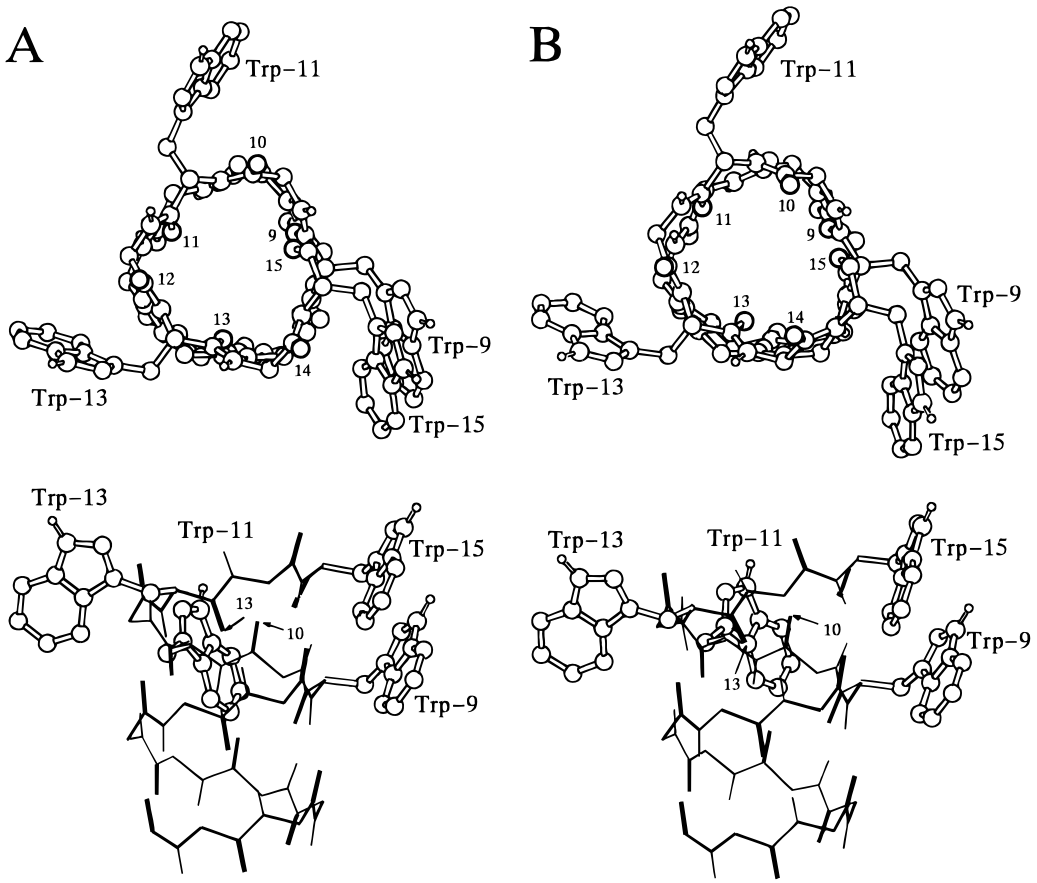

FIGURE 9: Two models for the gramicidin channel viewed from the channel mouth (top) and from the direction perpendicular to the channel axis (bottom): (A) model 1, (B) model 3. For the details of the models, see text. The amide C═O oxygens at positions 9−15 are drawn with thick open circles (top) or all the amide C═O bonds are represented with thick lines (bottom).

Table 2: Main-Chain Torsion Angles[a] in Models for the Gramicidin Ion Channel

	model 1[b]	model 2[c]	model 3[d]
ψ_8 (Val)	−109	−120	−110
ϕ_9 (Trp)	−131	−111	−130
ψ_{10} (Leu)	−105	−128	−140
ϕ_{11} (Trp)	−127	−109	−100
ψ_{12} (Leu)	−104	−119	−105
ϕ_{13} (Trp)	−134	−100	−125
ψ_{14} (Leu)	−93	−115	−140
ϕ_{15} (Trp)	−138	−108	−95

[a] Angles are given in degrees. [b] Ketchem et al. (*18*). [c] Tian et al. (*42*). [d] This work. The other torsion angles are the same as in model 1.

model 1. As a result, a number of (ϕ_i, ψ_{i-1}) sets were found to produce reasonable upward and downward shifts of the N_1H protons of Trp-11 and -13, respectively, with keeping the N_1H protons of Trp-9 and -15 around the original positions. One of such (ϕ_i, ψ_{i-1}) sets is listed in the third column of Table 2 and the d_{NH} values in the modified backbone conformation (model 3) are plotted with dots in Figure 7. The changes in water accessibility of Trp-11 and -13 upon binding of Na^+ are likely to arise from the shifts in d_{NH} indicated by arrows in the figure.

Figure 9 compares the main-chain structure and Trp orientations in model 3 with those in the original model 1. The Trp orientations with respect to the channel axis are almost identical in models 1 and 3. A marked difference between the two models is seen in the directions of the amide C═O bonds of Leu-10 and Trp-13. On going from model 1 (Figure 9A) to model 3 (Figure 9B), the angle of the C═O bond with respect to the channel axis changes from +19° to −19° for Leu-10 and from −22° to −34° for Trp-13, where the negative value indicates inclination toward the channel pore. Similar inward deflections of the C═O bonds of Leu-10 and Trp-13 were commonly observed for the other (ϕ_i, ψ_{i-1}) sets that produce d_{NH} consistent with the water accessibility data. The deflections of the C═O bonds and the axial shifts of Trp-11 and -13 must be highly correlated with each other.

^{13}C NMR studies have shown that the Na^+ binding site in the gramicidin channel is located at a position between the amide carbonyl carbons of Trp-11 and -13 (*46*, *47*). The distance of carbonyl carbon, measured along the helix axis, from the center of head-to-head dimer junction is 7.6 Å for Trp-11 and 8.8 Å for Trp-13 in model 3. Since electrostatic interactions between amide carbonyl oxygens and Na^+ are considered to play a key role in the Na^+ binding (*7*, *48*), we have examined the axial positions of carbonyl oxygens in model 3. Only two carbonyl oxygens, of Leu-10 (7.9 Å) and Trp-13 (7.8Å), are located within the expected range of Na^+ binding site but the other carbonyl oxygens are not. The two carbonyl oxygens of Leu-10 and Trp-13 are 5.5 Å apart across the channel pore and capable of accommodating an Na^+ ion (2.3 Å in diameter) in between. The deflection of the Leu-10 and Trp-13 C═O bonds toward the channel pore may be caused by the electrostatic interaction with the Na^+ ion. Similar deflections of C═O bonds near the bound cation have been predicted by molecular dynamics calculations (*49*, *50*). It is very likely that the binding of Na^+ to the gramicidin channel induces a conformational transition of

the peptide backbone accompanied by inward deflections of the Leu-10 and Trp-13 C═O bonds and concomitantly by positional shifts of Trp-11 and -13 along the channel axis. Model 3 may represent one such channel structure in the presence of cations. A conformational transition similar to that from model 1 to 3 illustrated in Figure 9 may occur upon cation binding. The synergetic motions of the C═O bonds and Trp indole rings suggest that Trp residues may take part in the orientational regulation of the C═O bonds that interact with the cations passing through the channel pore.

In summary, Raman spectroscopy combined with the deuterium labeling techniques has revealed the conformation, hydrophobic interaction, and water accessibility of each individual Trp residue of the gramicidin channel incorporated into phospholipid bilayers. Every Trp residue of the gramicidin channel has a $|\chi^{2,1}|$ angle of 94° ± 6° and is involved in strong hydrophobic interactions in both the cation-free and cation-bound states. Of particular importance in relation to the molecular mechanism of gramicidin ion transport is the finding that water accessibility significantly changes for Trp-11 and -13 upon cation binding. The changes of water accessibility are attributable to shifts of these Trp residues along the channel axis and are regarded as the first experimental evidence for a cation-induced conformational transition of the gramicidin channel backbone. The present study has demonstrated the utility of Raman spectroscopy in the analysis of water accessibility to Trp residues in membrane environments. Similar analysis may provide unique information on the structure and dynamics of other peptides and proteins bound to membranes.

ACKNOWLEDGMENT

We are grateful to the late Professor I. Harada for helpful discussions at an early stage of this work and to Dr. T. Yoshimitsu for expert technical assistance in peptide synthesis.

REFERENCES

1. Hladky, S. B., and Haydon, D. A. (1972) *Biochim. Biophys. Acta 274*, 294−312.
2. Myers, V. B., and Haydon, D. A. (1972) *Biochim. Biophys. Acta 274*, 313−322.
3. Rosenberg, P. A., and Finkelstein, A. (1978) *J. Gen. Physiol. 72*, 341−350.
4. Sarges, R., and Witkop, B. (1964) *J. Am. Chem. Soc. 86*, 1862−1863.
5. Killian, J. A. (1992) *Biochim. Biophys. Acta 1113*, 391−425.
6. Busath, D. D. (1993) *Annu. Rev. Physiol. 55*, 473−501.
7. Urry, D. W. (1971) *Proc. Natl. Acad. Sci. U.S.A. 68*, 672−676.
8. Urry, D. W., Trapane, T. L., and Prasad, K. U. (1983) *Science 221*, 1064−1067.
9. Venkatachalam, C. M., and Urry, D. W. (1983) *J. Comput. Chem. 4*, 461−469.
10. Nicholson, L. K., and Cross, T. A. (1989) *Biochemistry 28*, 9379−9385.
11. Hing, A. W., and Schaefer, J. (1993) *Biochemistry 32*, 7593−7604.
12. Heitz, F., Spach, G., and Trudelle, Y. (1982) *Biophys. J. 39*, 87−89.
13. Prasad, K. U., Trapane, T. L., Busath, D., Szabo, G., and Urry, D. W. (1983) *Int. J. Pept. Protein Res. 22*, 341−347.
14. Trudelle, Y., and Heitz, F. (1987) *Int. J. Pept. Protein Res. 30*, 163−169.
15. Becker, M. D., Greathouse, D. V., Koeppe, R. E., II, and Anderson, O. S., (1991) *Biochemistry 30*, 8830−8839.
16. Takeuchi, H., Nomoto, Y., and Harada, I. (1990) *Biochemistry 29*, 1572−1579.
17. Hu, W., Lee, K.-C., and Cross, T. A. (1993) *Biochemistry 32*, 7035−7047.
18. Ketchem, R. R., Hu, W., and Cross, T. A. (1993) *Science 261*, 1457−1460.
19. Koeppe, R. E., II, Killian, J. A., and Greathouse, D. V. (1994) *Biophys. J. 66*, 14−24.
20. Hu, W., Lazo, N. D., and Cross, T. A. (1995) *Biochemistry 34*, 14138−14146.
21. Matthews, H. R., Matthews, K. S., and Opella, S. J. (1977) *Biochim. Biophys. Acta 497*, 1−13.
22. Bolin, D. R., Sytwu, I.-I., Humiec, F., and Meienhofer, J. (1989) *Int. J. Pept. Protein Res. 33*, 353−359.
23. Kisfaludy, L., and Schön, I. (1983) *Synthesis*, 325−327.
24. Fields, C. G., Fields, G. B., Noble, N. L., and Cross, T. A. (1989) *Int. J. Pept. Protein Res. 33*, 298−303.
25. Busath, D. D., Andersen, O. S., and Koeppe, R. E., II (1987) *Biophys. J. 51*, 79−88.
26. LoGrasso, P. V., Moll, F., III, and Cross, T. A. (1988) *Biophys. J. 54*, 256−267.
27. Killian, J. A., Prasad, K. U., Hains, D., and Urry, D. W. (1988) *Biochemistry 27*, 4848−4855.
28. Bouchard, M., and Auger, M. (1993) *Biophys. J. 65*, 2484−2492.
29. Greathouse, D. V., Hinton, J. F., Kim, K. S., and Koeppe, R. E., II (1994) *Biochemistry 33*, 4291−4299.
30. Huang, C., Lapides, J. R., and Levin, I. W. (1982) *J. Am. Chem. Soc. 104*, 5926−5930.
31. Miura, T., Takeuchi, H., and Harada, I. (1989) *J. Raman Spectrosc. 20*, 667−671.
32. Maruyama, T., and Takeuchi, H. (1995) *J. Raman Spectrosc. 26*, 319−324.
33. Harada, I., Miura, T., and Takeuchi, H. (1986) *Spectrochim. Acta, Part A 42*, 307−312.
34. Miura, T., Takeuchi, H., and Harada, I. (1988) *Biochemistry 27*, 88−94.
35. Takeuchi, H., and Harada, I. (1986) *Spectrochim. Acta, Part A 42*, 1069−1078.
36. Takesada, H., Nakanishi, M., Hirakawa, A. Y., and Tsuboi, M. (1976) *Biopolymers 15*, 1929−1938.
37. Price, H. D., and Thompson, T. E. (1969) *J. Mol. Biol. 41*, 443−457.
38. Deamer, D. W., and Bramhall, J. (1986) *Chem. Phys. Lipids 40*, 167−188.
39. Momany, F. A.,McGuire, R. F., Burgess, A. W., and Scheraga, H. A. (1975) *J. Phys. Chem. 22*, 2361−2381.
40. Arseniev, A. S., Lomize, A. L., Barsukov, I. L., and Bystrov, V. F. (1986) *Biol. Membr. 3*, 1077−1104.
41. Hu, W., and Cross, T. A. (1995) *Biochemistry 34*, 14147−14155.
42. Masotti, L., Cavatorta, P., Sartor, G., Casali, E., and Szabo, A. G. (1986) *Biochim. Biophys. Acta 862*, 265−272.
43. Tian, F., Lee, K.-C., Hu, W., and Cross, T. A. (1996) *Biochemistry 35*, 11959−11966.
44. Akutsu, H., and Seelig, J. (1981) *Biochemistry 20*, 7366−7373.
45. Lis, L. J., Kauffman, J. W., and Shriver, D. F. (1975) *Biochim. Biophys. Acta 406*, 453−464.
46. Separovic, F., Gehrmann, J., Milne, T., Cornell, B. A., Lin, S. Y., and Smith, R. (1994) *Biophys. J. 67*, 1495−1500.
47. Urry, D. W., Prasad, K. U., and Trapane, T. L. (1982) *Proc. Natl. Acad. Sci. U.S.A. 79*, 390−394.
48. Jong, N., Prasad, K. U., and Urry, D. W. (1995) *Biochim. Biophys. Acta 1238*, 1−11.
49. Mackay, D. H. J., Berens, P. H., Wilson, K. R., and Hagler, A. T. (1984) *Biophys. J. 46*, 229−248.
50. Jordan, P. C. (1990) *Biophys. J. 58*, 1133−1156.

BI9710838